ELSEVIER

Synthetic Metals 84 (1997) 501-506

SYNTHETIC METALS

Absorption and Luminescence of Pyridine-Based Polymers

S. W. Jessen,[a] J. W. Blatchford,[a] L.-B. Lin ,[b] T. L. Gustafson ,[c]J. Partee, [c]J. Shinar, [d] D.-K. Fu,[d] M. J. Marsella,[d]T. M. Swager,[d] A. G. MacDiarmid,[d] and A. J. Epstein[a,b]

[a]*Department of Physics and* [b]*Department of Chemistry, The Ohio State University, Columbus, Ohio, 43210-1106, USA*

[c]*Department of Physics, Iowa State University, Ames, IA 50011, USA*

[d]*Department of Chemistry, University of Pennsylvania, Philadelphia, Pennsylvania, 19104-6323, USA*

Abstract

We summarize the low energy photophysics of the pyridine-based polymers poly(*p*-pyridine)(PPy), poly(*p*-pyridyl vinylene) (PPyV) and copolymers made up of PPyV and poly(*p*-pheneylene vinylene) (PPyVPV). The absorption and luminescence properties are morphology dependent. The primary photoexcitations within these polymers are singlet excitons which may emit from individual chains following a random walk to lower energy segments, depending upon the excitation energy. Films display redshifted absorption and emission properties with a decrease in photoluminescence efficiency which can be attributed to aggregate formation in comparison to powder and solution forms. Photoinduced absorption (PA) studies show direct conversion of singlet to triplet excitons on the ps time scale. Polaron signatures and the transition between triplet exciton states are seen in powder forms using ms PA techniques. Film forms display only a polaron signature at millisecond times indicating that morphology plays a key role in the long-time photophysics for these systems. Photoluminescence detected magnetic resonance studies also have signatures due to both polarons and triplet excitons. The size of the triplet exciton is limited to a single ring suggesting that the triplet exciton may be trapped by extrinsic effects.

Keywords: Optical absorption and emission spectroscopy, photoinduced absorption spectroscopy, optically detected magnetic resonance, other conjugated and/or conducting polymer.

Introduction

The advent of poly(*p*-phenylene vinylene) (PPV) as an efficient emissive layer within light emitting devices (LEDs) has opened many developments within the conjugated polymer community over the last several years [1]. In particular, researchers have focused upon making longer lasting and more efficient polymer LEDs. One means of achieving such a goal is by understanding the underlying photophysical processes of the luminescent conjugated polymers.

Many discussions have centered around the nature of the primary photoexcitations within these systems (particularly the (poly-arylenes)). Some authors maintain that nonlinear excitations such as polarons and polaron-excitons are the primary excitations [2-6]. Others claim that Coulombically bound electron-hole pairs or excitons are the primary photoexcitations [7-13]. Within these latter models, further argument centers around the strength of the electron-electron interactions with values ranging from 0.4 - 1.1 eV [7-13].

Numerous studies on PPV have concentrated on varying the sidegroups along the polymer chain in order to change the electronegativity, the nature of the exciton, or to enhance the solubility of the polymer in order to fabricate more efficient devices [14-15]. In these cases, the backbone of the polymer was unaltered therefore leaving little changes in the photophysical properties of these polymers compared to PPV. In addition to being more electronegative and soluble in weak acids in its unaltered form, the incorporation of a nitrogen heteroatom to the backbone of the polymer chain can lead to changes in the low energy photophysics of the pyridine-based polymers poly(*p*-pyridine) (PPy) and poly(*p*-pyridyl vinylene) (PPyV) in comparison to their phenylene-based counterparts.

We present an overview of the photophysical properties of the pyridine-based polymers PPy, PPyV and copolymers made up of PPyV and PPV ($PPyVP(R)_2V$) with various sidegroups used to keep the polymer chains well separated and soluble in differing solvents. From absorption and luminescence studies, the primary excitations in pyridine-based polymers are singlet excitons. In addition, there are conformational differences between samples of differing morphology: films cast from either formic acid or tetrahydrofuran (THF) solution are susceptible to aggregate formation (regions where both the ground and excited state wave functions can be delocalized over several chains). Photoinduced absorption (PA) on powder, solution and film samples of PPyV further support the exciton picture, showing enhanced triplet exciton production in powders in addition to direct observance of singlet to triplet exciton conversion on the picosecond time scale. Through millisecond PA, triplet excitons and polarons are determined to be the dominant long-lived species. The volume density of triplet excitons being larger in powders than films, once again supporting enhanced triplet production in this morphology. Photoluminescent detected magnetic resonance (PLDMR) studies support the ms PA assignments in both powders and films, yielding that the spatial extent of the triplet exciton is ~ 2.8 Å. We propose this small size to be due to extrinsic effects which act to localize to the triplet exciton to a single ring.

PII S0379-6779(96)03994-X

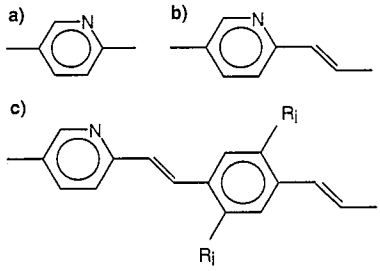

Fig. 1. Schematic structure of a) PPy, b) PPyV and c) PPyVP(R_i)$_2$V.

Experimental Procedures

The polymer samples, schematically shown in Fig. 1, were synthesized as powders [16-18]. In this paper, we refer to three different forms of the pyridine-based polymers: powder, solution and film. "Powder" refers to the as-precipitated solid form obtained directly after the synthesis has occurred. These powders could then be dissolved to form solutions of various concentrations. Films could then by either drop- or spin- cast onto quartz substrates from the solution. The optical studies of the powder forms were performed by dispersing the polymer in KBr (~0.02%-0.04% by mass) and pressing the subsequent mixture into a pellet form. Solutions were prepared by dissolving the polymer in formic acid (HCOOH), for PPyV and PPy, and spectroscopic grade THF, for the copolymers.

The optical absorption measurements were made using a Perkin Elmer Lambda 19 UV/Vis/NIR spectrometer. The photoluminescence spectra (cw) were measured with either a SPEX Fluorolog or a PTI Quantamaster fluorometer. Details of the time-resolved photoluminescence (PL) measurements, PL efficiencies, ms and ps PA, as well as the optically detected magnetic resonance (ODMR) apparati are discussed elsewhere [19-22].

Absorption and Photoluminescence

Figure 2 compares the optical absorption spectra of solution, powder and film forms of PPy and PPyV with that of each of the copolymers for energies less than 4.5 eV. Examining the solution and powder spectra for PPyV, there is little difference in the optical absorption: the absorption edges ~ 2.5 eV with maxima ~ 3.0 eV. Film spectra have a longer tail into the IR (absorption edge ~ 2.4 eV) and peak around 3.0 eV indicating that there is little overall change in the distribution of conjugation sites when comparing to powder and solution forms. As will be discussed later, the longer tail into the IR is a result of the formation of aggregate states within the polymer sample [19,23]. Each of the three copolymers, as well as PPy, behave similarly. Additionally, the photoluminescence excitation (PLE) spectra for films compared to powder and solution forms of each polymer are redshifted, peaking at an energy within the tail of the absorption and very near the peak in the PL [19]. The latter forms have PLE spectra lying very near the peak in the lowest lying absorption feature with a larger apparent Stokes shift. The copolymers show little overall change in the low energy photophysics with respect to the parent polymers. The only observed differences are a redshift of the direct and photoinduced absorption and PL by ~0.2-0.4 eV and carbonyl formation which quenches the PL and PA signals of the copolymer with the alkoxy sidegroup, (PPyVP($OC_{16}H_{33}$)$_2$V) [23,24], similar results have been seen for alkoxy derivatives of PPV [25].

The photoluminescence for dilute solution (< 10^{-5} M), powder and film forms of PPyV (top), PPy (middle) and a representative copolymer (bottom) are shown in Figure 3. In each of the polymers the powder and solution spectra are similar; while the film spectrum is redshifted by as much as 0.5 eV indicating that emission in films comes from lower energy sites. The PL efficiencies of solutions are quite high for the copolymers (~70-90%), but are lower for PPyV and PPy (~10%-20%). Additionally, the PL in solutions is very nearly independent of concentration, suggesting that excimer formation is not occurring. The PL decays are almost single exponential (> 90%) and are independent of wavelength in all the materials except PPy where there is a slight redshift with time. The radiative lifetime is found to be ~1-2 ns for the polymers studied [19].

The large apparent Stokes shift (~0.5 eV) between absorption and emission spectra in solution and powder forms stems from exciton migration to lower energy segments followed by radiative or nonradiative decay. Site selective fluorescence studies yield an intrinsic Stokes shift of ~60 meV [19], a result comparable to that found by Bässler and coworkers for PPV [26-27] indicating that exciton migration is applicable to these systems. In addition, Huang-Ryss analysis on PPyVP($OC_{16}H_{33}$)$_2$V yields a relaxation energy ~ 86 meV for the pyridine-based polymers with strong coupling to the 1300 cm^{-1} C=C stretching mode of the vinylene unit [19], indicating a relatively weak geometrical relaxation for the singlet exciton.

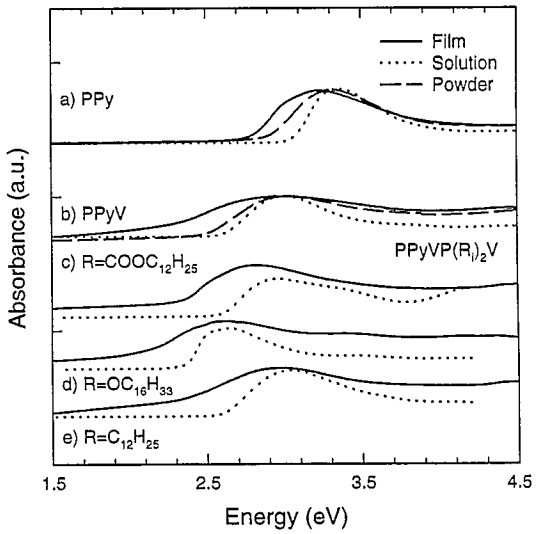

Fig 2. Optical absorbance in film (solid), solution (dotted) and powder (dashed) forms of a) PPy, b) PPyV, c) PPyVP($COOC_{12}H_{25}$)$_2$V, d) PPyVP($OC_{16}H_{33}$)$_2$V and e) PPyVP($C_{12}H_{25}$)$_2$V.

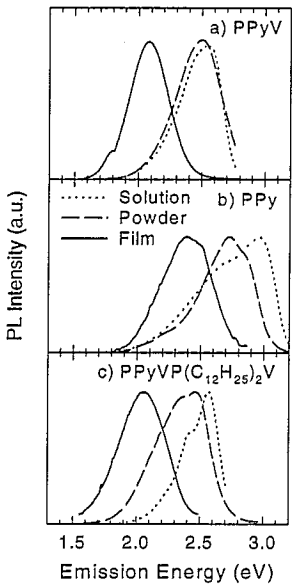

Fig. 3. Photoluminescence of solution (dotted), powder (dashed) and film (solid) forms of a) PPyV, b) PPy and c) $PPyVP(C_{12}H_{25})_2V$ [19].

Corresponding with the increased oscillator strength in the IR absorption, in all cases the film PL is redshifted with respect to the solution PL by ~ 0.5 eV. Furthermore, the internal quantum efficiencies for films are quite low, ~ 1/3 - 1/2 of the solution values [19]. Aggregate sites act to reduce the luminescence efficiency of films, as the radiative lifetime of aggregate excitons is longer than that of intrachain or solution-like excitons. The powder PL spectra once again strongly resembles that of solutions. These results taken in conjunction with the absorption results indicate that both the absorption and luminescence are dependent upon the morphology of the sample. The degree of aggregation in film samples being dependent upon the type of solvent used and the method of preparation [19].

Aggregate formation in pyridine-based polymers is further supported by recent near-field scanning optical microscopy (NSOM), a technique which allows direct spatial imaging of absorption and emission in polymer films to a resolution of 100 nm [23,28-30]. Emission in PPyV films is localized to partially aligned regions of domain size ~ 200 nm indicating that aggregates most likely form within these aligned regions. The evolution of the photoluminescence within film forms of the pyridine-based polymers is shown for a representative polymer in Fig. 4. The cw PL of solution (dotted) and film (solid) forms are also shown for clarity. At "0 ps" delay time (actually < 50 ps due to instrument resolution), the PL consists of both a solution-like (intrachain) and film-like (aggregate) component suggesting that at least half the "initial" emission is a result of aggregate sites. Within 1 ns (triangle), the emission is entirely aggregate-like and the intrachain excitons have migrated to the aggregate sites. Examining the time decay of the PL, the radiative lifetime for the aggregate excitons is ~ 8 ns [19]. The longer radiative lifetime allows the excitons to find other nonradiative decay pathways resulting in a lower quantum efficiency for films, as discussed above [19]. These results

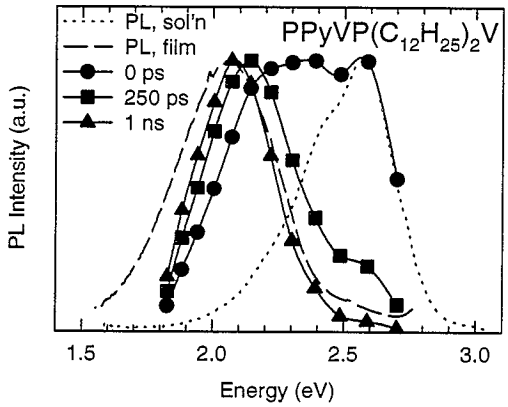

Fig. 4. Evolution of the PL of $PPyVP(C_{12}H_{25})V$ with 0 ps (circle), 250 ps (square) and 1 ns (triangle) delay times for $PPyVP(C_{12}H_{25})_2V$ films.

have immediate implications for LEDs since higher efficiency devices are desired.

Photoinduced Absorption

Figure 5 shows the picosecond (ps) to millisecond (ms) photoinduced absorption (PA) for powder and solution forms of PPyV. For the ps PA technique, pumping was at 2.8 eV with the sample at room temperature, but under vacuum. The fs and ps PA at 0 ps time delay for powder and solution forms has three photoinduced features: a PA feature around 1.5 eV (at the limit of the detector) attributed to a transition to a higher energy state of intrachain singlet excitons, photoinduced bleaching (PB) from 2.2 - 2.5 eV as a result of stimulated emission (SE) of singlet excitons and PB of the absorption edge for energies greater than 2.5 eV. The ms PA spectrum for PPyV powders using probe energies greater than 1.5 eV has two discernible features: PA at 1.8 eV attributed to the transition between triplet exciton states with lifetimes around 540 μs and PB for energies greater than 2.5 eV, again consistent with the onset of absorption.

By monitoring the decay of the ps PA signal at various energies, the evolution of the PA signal varies depending upon the morphology of the sample [21], as displayed in Fig. 6. For solutions of PPyV, the PA at 1.4 eV decays single-exponentially matching the PL decay up to 1.3 ns. The 1.9 eV and 2.2 eV PA deviate from the PL decay for delay times greater than 300 ps indicating the existence of a longer-lived species on the ps time scale. Concentration and pump intensity dependent ps PA studies on solutions indicate that the long-lived signal is intrachain in nature. In powders, the 1.9 eV and 2.2 eV signals are immediately swamped by the longer-lived species. The rise of these features are correlated with the decay of 1.4 eV PA feature indicating that the longer-lived state is directly created from the singlet exciton. In addition, the powder signal is an order of magnitude larger than the solution signal indicating that the longer-lived signal has a larger volume density in powders than solutions. Film forms of PPyV, once again, have a longer-lived component at 1.9 eV

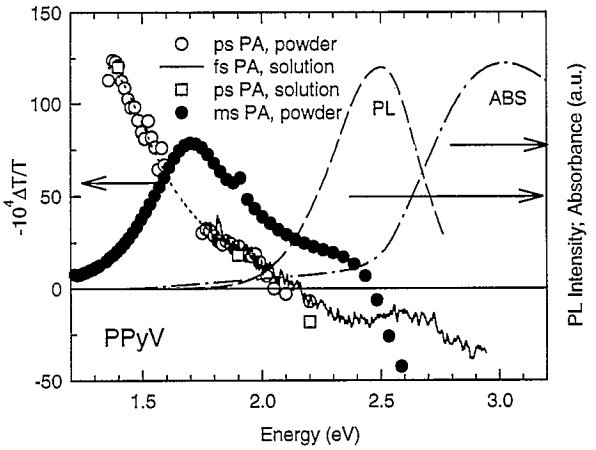

Fig. 5. The absorption (dot-dashed), photoluminescence (dashed) and photoinduced absorption spectra of solution and/or powder forms of PPyV; ps PA powder (hollow circle), fs PA solution (solid line), ps PA solution (hollow square), and ms PA (circle). The dotted line is a fit to the ps PA (adapted from [21]).

with the magnitude of the signal similar to that found in solutions.

Fig. 7 compares the spectral response of the ps PA for powders at 1 ns delay time (diamonds) to the ms PA of powder (solid) and film forms (dashed) of PPyV. The chopper was set to 15 Hz with a pump energy of 2.71 eV and incident intensity of 150 mW/cm^2 upon a sample cooled to 80 K. The solution ms PA could not be measured on the current system. As can be seen, the spectral response of the ps PA correlates nicely with the triplet-triplet transition at 1.8 eV indicating that the longer-lived signal discussed above is associated with a triplet exciton. In addition, there is a lower energy, and much weaker feature in the powder ms PA near 0.9 eV. This feature is more clearly seen by examining the quadrature component of the signal, as seen in the inset. The ms PA spectrum for film form differs from the powder form in that two discernible features are seen near 1.0 eV and 1.8 eV and the signal is about an order of magnitude less than the triplet exciton feature of powders, but is the same intensity as the lower energy feature seen in powders. The observation of photoinduced infrared active vibrational (IRAV) modes near the same locations in both powder and film forms which correlate to the 0. 9 eV.feature in powder and both of the film features through parameter dependent measurements indicate that these features are associated with polarons [20]. The origin of the aggregate formation in films could be a result of liquid-crystal order. It has been demonstrated that PPyVPV samples exhibit a sanidic or board-like liquid-crystalline phase at certain temperatures [18]. PPyVPV may also be liquid crystalline in solution in a variety of solvents [19]. Powders are precipitated from a solvent in which they are poorly soluble. The resultant sample has a disordered, tangled, "coil-like" morphology which can support a variety of 'extrinsic' effects. Films are dissolved from a concentrated solvent in which the sample dissolves well, leading to liquid crystalline order. The liquid crystalline order

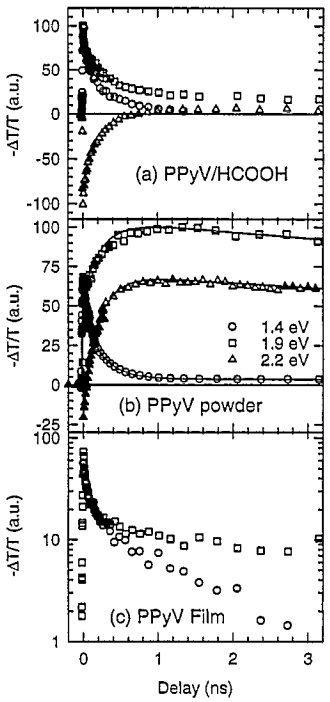

Figure 6. The decay of the ps PA monitored at 1.4 eV (circle), 1.9 eV (square) and 2.2 eV (triangle) for a) HCOOH solution, b) powder and c) film forms of PPyV. The sample were pumped at 2.8 eV.

likely remains as the solvent evaporates upon film formation leading to regions of closely packed chain alignment and order.

The apparent lack of a triplet exciton signal and the creation of aggregate states in films stem from these more ordered regions within the polymer sample. The powder form likely has many torsional defects which mix (n,π^*) and (π,π^*)

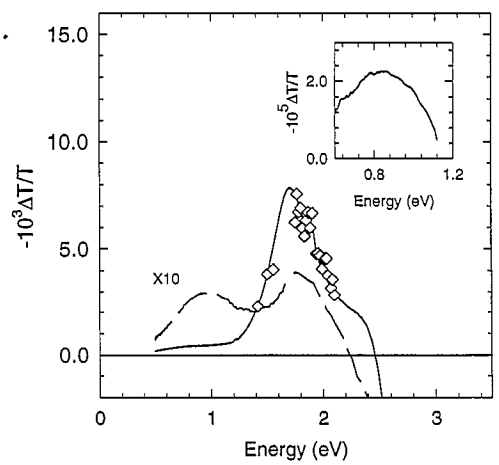

Figure 7. Comparison of the ps PA of powder at 1 ns time delay (diamonds) to ms PA of powder (solid) and film (dashed) forms of PPyV. The inset shows the quadrature signal for a powder sample.

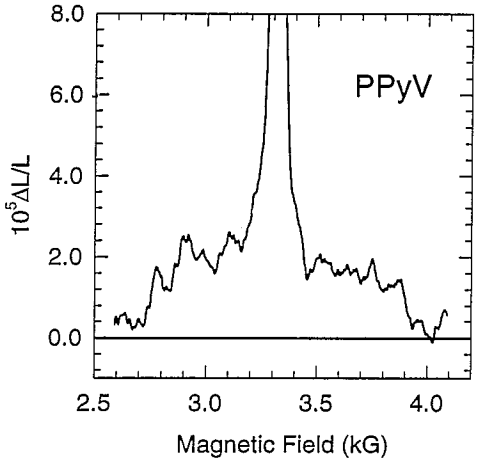

Fig. 8. The PLDMR full-field triplet powder pattern of powder forms of PPyV.

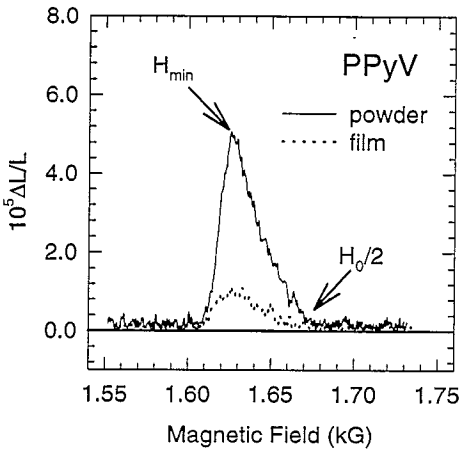

Fig. 9. The PLDMR half-field triplet powder pattern for powder forms of PPyV powders (solid) and films (dotted).

states, as predicted by quantum chemical calculations [31], and allow enhanced triplet exciton production through first order spin-orbit interaction [32].

Photoluminescence Detected Magnetic Resonance

The photoluminescence magnetic resonance (PLDMR) for PPyV powder cooled to 15 K at full-field is shown in Fig. 8. The pumping energy was 2.71 eV with the μ-wave chopped at 100 kHz and incident power of 811 mW/cm^2. A broad (~1200 G wide), PL enhancing triplet powder pattern is symmetrically distributed around a 5 - 20 G wide, PL enhancing polaron resonance at the full-field value, ~ 3.35 kG. The polaron resonance decreased in intensity, yet remained enhancing for excitation energies up to 3.31 eV, consistent with behavior in poly(*p*-phenylene ethynylene) [33]. Similar results are seen for the PPyVPV copolymers. These results support the production of triplet excitons and polarons observed using ms PA.

The half-field PLDMR signals for the PPyV powder and film forms are shown in Fig. 9. The experimental parameters are the same as discussed above. An asymmetric powder pattern is observed with onset at the half-field value $H_0/2$ (~ 1.68 kG) and peak at H_{min}, the minimum value at which a $\Delta m_s = \pm 2$ can occur [34]. The magnitude and full-width at half-maximum of the signal in powders are similar in each polymer studied indicating that the distribution in the zero-field splitting parameters, D and E, and the separation between spin states are similar [35]. In addition, a half-field pattern is observed in film forms of PPyV, but is an order of magnitude less than powder forms.

We can estimate the separation between spin states from the following relations:

$$D^* = \frac{\sqrt{D^2+3E^2}}{g\beta} = \sqrt{3\left[\left(\frac{H_0}{2}\right)^2 - H_{min}^2\right]}$$

$$r_{UB} \approx 24.1\sqrt[3]{D^*},$$

where D, E are the zero-field splitting parameters, g the Landé g-factor, β the Bohr magneton, H_0 and H_{min} defined as above [34,36]. In all cases, the spatial extent of the triplet exciton is roughly estimated to be ~ 2.8 Å or about the size of a benzene ring, suggesting that the triplet exciton is localized to a single unit. These results are inconsistent with calculations which suggest that the spatial extent of singlet and triplet excitons should be several units long [31]. We suggest that the triplet excitons observed using PLDMR and likely in the PA experiments as well are trapped by extrinsic effects such as conjugation defects and interchain effects which localize the long-lived exciton to a single ring [35]. The film PLDMR signal is an order of magnitude less than the powder signal in PPyV. As discussed above, films are susceptible to aggregate formation which tends to align the chains making them more planar thereby reducing the number of torsional defects and possibly the number of sites which may act to trap long-lived triplet excitons.

Conclusions

Upon absorption of a photon of sufficient energy, the primary photoexcitations in pyridine-based polymers are singlet excitons. Both the absorption and luminescence are broad and devoid of any clear features as a result of inhomogeneous broadening due to disorder. Using site selective fluorescence and Huang-Ryss type analyses, an intrinsic Stokes shift of ~60 meV with very little lattice relaxation (~86 meV) are found, respectively. The low energy photophysics of powder and solution forms are similar. Films are susceptible to aggregate formation, as seen using absorption, luminescence and NSOM techniques. The radiative lifetime of the aggregate exciton is longer than the intrachain exciton found in solution and powder forms resulting in a decrease in luminescence efficiency for films. PA studies show additional morphology dependent results with enhanced triplet exciton production in powder compared to film forms due to mixing of (n,π*) and (π, π*) states. The PLDMR determined spatial extent of the triplet exciton found on the μs-ms time scale is ~ the size of a benzene

ring suggesting that extrinsic (*e.g.*, interchain) effects may trap the exciton within a single ring.

Acknowledgments:

This work was supported in part by the Office of Naval Research.

References:

1. J. H. Burroughes, D. D. C. Bradley, A. R. Brown, R. N. Marks, K. Mackay, R. H. Friend, P. L. Burns, and A. B. Holmes, Nature **347**, 539 (1990).
2. A. J. Heeger, S. Kivelson, J. R. Schrieffer, and W. P. Su, Rev. Mod. Phys. **60**, 781 (1988).
3. K. Fesser, A. R. Bishop, and D. K. Campbell, Phys. Rev. B **27**, 4804 (1983).
4. Y. Furukawa, Synth. Met. **69**, 629 (1995).
5. T. W. Hagler, K. Pakbaz, and A. J. Heeger, Phys. Rev. B. **51**, 14199 (1995).
6. K. Pakbaz, C. H. Lee, A. J. Heeger, T. W. Hagler, and D. McBranch, Synth. Met. **64**, 295 (1994).
7. Yu. N. Gartstein, M. J. Rice, and E. M. Conwell, Phys. Rev. B **51**, 5546 (1995).
8. P. Gomes da Costa and E. M. Conwell, Phys. Rev. B **48**, 1993 (1993).
9. D. Beljonne, Z. Shuai, R. H. Friend, and J. L. Brédas, J. Chem. Phys. **102**, 2042 (1995).
10. M. Chandross, S. Mazumdar, S. Jeglinski, X. Wei, and Z. V. Vardeny, Phys. Rev. B **50**, 14702 (1994).
11. J. M. Leng, S. Jeglinski, X. Wei, R. E. Benner, Z. V. Vardeny, F. Guo, and S. Mazumdar, Phys. Rev. Lett. **72**, 156 (1993).
12. S. Abe, J. Yu, and W. P. Su, Phys. Rev. B **45**, 8264 (1992).
13. Z. G. Soos, S. Ramesesha, and D. S. Galvão, Phys. Rev. Lett. **71**, 1609 (1993).
14. M. Fahlman, M. Lögdlund, S. Stafström, W. R. Salaneck, R. H. Friend, P. L. Burn, A. B. Holmes, K. Kaeriyama, Y. Sonoda, O. Lhost, F. Meyers, and J. L. Brédas, Macrom. **28**, 1959 (1995).
15. F. Meyers, A. J. Heeger, and J. L. Brédas, J. Chem. Phys. **97**, 2750, (1992).
16. M. J. Marsella, D.-K. Fu and T. M. Swager, Adv. Mater. **7**, 145 (1995).
17. T. Yamamoto, T. Marruyama, Z. Zhou, T. Ito, T. Fukuda, Y. Yoneda, F. Begum, T. Ikeda, S. Sasaki, H. Takezoe, A. Fukuda, and K. Kubota, J. Am. Chem. Soc. **116**, 4832 (1994).
18. D.-K. Fu, M. J. Marsella, and T. M. Swager, Polym. Preprints **36**, 585 (1995).
19. J. W. Blatchford, S. W. Jessen, L.-B. Lin, T. L. Gustafson, A. J. Epstein, D.-K. Fu, H.-L. Wang, T. M. Swager, and A. G. MacDiarmid, Phys. Rev. B, *in press*.
20. S. W. Jessen, J. W. Blatchford, Y. Z. Wang, D. D. Gebler, L.-B. Lin, T. L. Gustafson, A. J. Epstein, T. Yuzawa, H. Hamaguchi, D.-K. Fu, M. J. Marsella, T. M. Swager, and A. G. MacDiarmid, *submitted for publication*.
21. J. W. Blatchford, S. W. Jessen, L.-B. Lin, J.-J. Lih, T. L. Gustafson, T. M. Swager, A. G. MacDiarmid, and A. J. Epstein, Phys. Rev. Lett. **76**, 1513 (1996).
22. S.W. Jessen *et al.*, *to be published*.
23. J. W. Blatchford, T. L. Gustafson, A. J. Epstein, D. A. Vanden Bout, J. Kerimo, D. A. Higgins, P. F. Barbara, D.-K. Fu, T. M. Swager, and A. G. MacDiarmid, Phys. Rev. B, *in press*.
24. S. W. Jessen, Ph. D. Thesis, The Ohio State University, 1996.
25. F. Papadimitrakopoulos, K. Konstadinidis, T. M. Miller, R. Opila, E. A. Chandross, and M. E. Galvin, Chem. Mater. **6** 1563 (1994).
26. U. Rauscher, L. Schutz, A. Greiner, and H. Bässler, J. Phys.: Condens. Matter **1**, 9751 (1989).
27. U. Rauscher, H. Bässler, D. D. C. Bradley, and M. Hennecke, Phys. Rev. B **42**, 9830 (1990).
28. E. Betzig, J. K. Trautman, T. D. Harris, J. S. Weiner, and R.L. Kostelak, Science **251**, 1468 (1991).
29. E. Betzig and J. K. Trautman, Science **257**, 189 (1992).
30. D. A. Higgins and P. F. Barbara, J. Phys. Chem. **99**, 3 (1995).
31. J. W. Blatchford, T. L. Gustafson and A. J. Epstein, J. Chem. Phys., *in press*.
32. M. El-Sayed, J. Chem. Phys. **38**, 2834 (1963).
33. J. Shinar, *Handbook of Organic Conductive Molecules and Polymers*, (J. Wiley and Sons, Inc., New York, 1996), Ch. 22.
34. S. P. McGlynn, T. Azumi, and M. Kinoshita, *Molecular Spectroscopy of the Triplet State*, (Prentice-Hall, Inc., Engle Woods Cliffs, N. J., 1969).
35. J. Partee, J. Shinar, S. W. Jessen, A. J. Epstein, W. Graupner, and G. Leising, *to be published*.
36. S. Swanson, J. Shinar, and K. Yoshino, Phys. Rev. Lett. **65** (1990) 1140.